Variability of the internal wave continuum: study of 2500 worldwide seasonal to inter-annual time series

Arnaud Le Boyer, and Matthew H. Alford

Scripps Institution of Oceanography,
University of California San Diego
aleboyer@ucsd.edu

Abstract

Internal Gravity Waves (IGW) span time scales between the inertial frequency f ($\sim$1 day^{-1}) and buoyancy frequency N ($\sim$15 min^{-1} in the thermocline). The level of the continuum (defined as all frequencies apart from near-inertial and tidal) is related to small scale mixing, but its energy sources are poorly understood. We hypothesize that the continuum receives energy only from the wind, the tides and the mesoscale turbulence via the generation of near inertial waves (NIW), internal tides (IT) and lee-waves. These then exchange energy with each other and the continuum via triad interactions. If this hypothesis is correct, the kinetic energy (KE) within the continuum should covary with KE of the sources, possibly with a lag. Here, we investigate this relationship within a database of 2500 globally distributed, moored current-meter records (deployed on 697 separate moorings). The time evolution of the KE of the sources and continuum is obtained by computing spectra using sliding 30-days multitaper spectral windows. As a first approximation, the sources are defined as the diurnal and semi-diurnal tidal components and the wind. The preliminary results suggest that, contrary to the conventional view that IGW continuum is constant in space and time, the level varies by a factor of 10 at typical moorings. Additionally, parameters such as the energy level and the correlation between the sources and the continuum are classified and presented as function of geographical position and season.

1 Introduction

Internal gravity waves (IGW) provide a pathway to dissipation of the ocean's mechanical energy (Frankignoul and Joyce, 1979; Watson, 1985; Henyey et al., 1986; Gregg, 1989). For time scales from the inertial frequency f ($\sim$ 1 day^{-1}) to the buoyancy frequency N(15 min)$^{-1}$ in the thermocline), these waves continuously transfer energy to smaller scales via wave-wave interactions. The energy transfer through scales shapes the IGW continuum which is well described by the analytical expression of Garrett and Munk (1979) (henceforth GM79). This expression estimates the shape and slope of the continuum assuming the independence of its frequency and wavenumber in a near steady state of the IGW spectrum. The parameters in GM79 are tuned to fit the high frequency part of the kinetic energy (KE) spectrum of a great number of observations. However, Pinkel (1985) shows observations of a wavenumber spectrum varying with frequency contradicting the assumption made in GM79. Nowadays, the mechanisms driving the behavior of the continuum are still poorly understood mainly because these processes span a large range of time and spatial scales and, therefore, require a great number of long term (>month) time series sampled at high frequency to cover the global variability of both the dissipation and the energy sources of the continuum.

The relationship between the turbulent mesoscale activity and the IGW continuum has been developed (Watson, 1985) but is still a work in progress. The theoretical frame-

work developed in Nikurashin and Ferrari (2010) shows that the observed mixing rates can be sustained by internal waves generated by geostrophic motions flowing over bottom topography. This result is supported by both direct observations and numerical simulations. Clement et al. (2016) recently observed that IGW generation increases with the mesoscale activity via eddy-topography interaction for intense radial eddy velocities, and Nikurashin et al. (2014), using a model with realistic 3D topography, showed that 0.15 TW is transferred from geostrophic motions into IGW generation. The wind and the tides are additionally known to be sources of IGWs. The variability of the wind forces convergent and divergent flows in the surface mixed layer that trigger near inertial waves (NIW). These waves have a strong signature on the vertical shear and thus are likely to enhance the mixing at the interface of isopycnal layers. The surface tides also force internal tides (IT) that are generated where the topographic slope is similar to the slope of the IGW that the fluid can locally support. The IT characteristics (frequency and wavelength) depend on the forcing frequency and the background stratification.

Since the wind forces motions at NI frequencies, the lowest frequencies of the IGW spectrum, the NI peak is expected to be more energetic than a considerable portion of the mesoscale turbulence on a global scale. The tides can locally be much more energetic than both mesoscale and NI motions. Consequently, it is very likely that the IGW perturb proxies usually used to describe the baroclinic mesoscale activity like the sea surface anomaly. Thus, any projects like the SWOT (Surface Water Ocean Topography) project, that aim to measure the sea surface height, will be a great source of information on the IGWs dynamic. Once the community will be able to extract the IGW signal from these measurements, they will also provide a source of information on the dissipation in the global ocean since we might be able to track the temporal and spatial variability of the KE sources that shape the IGW Continuum.

These three sources of KE (mesocale activity, NIW and IT) might act on the IGW continuum in different ways: the mesoscale activity via lee-wave generation (Nikurashin and Ferrari, 2010) and mesoscale diffusion (Watson, 1985) and NIW and IT via triad interaction and internal wave breaking. A simple approach would expect the KE in the IGW continuum to rise and fall as a linear combination of the variability of the sources. This hypothesis implies that the KE linearly cascades toward dissipation scales through wave-wave interactions on a time scale of a 2-3 of days. Within this framework, the sources would either increase the energy flux through scales (i.e: increasing the slope of the continuum) or simply increase the overall KE level of the continuum with a constant energy flux.

Our goals are to understand shape/level variations in the IGW continuum and how they relate to mixing, understand its relationship to KE sources and understand its variability in the SSH signal. As a first step, this study starts to map the baroclinic activity of the IGW in contrast with its sources.

2 Data and Methods

Our work follows Alford (2003) and Alford and Whitmont (2007) studies which used data from more than 2500 historical moorings. We selected time series with lengths greater than 30 days and a sampling period of less than 3 hours. Figure 1 shows the 697 locations that meet these criteria. Alford and Whitmont (2007) already note the bias induced by the strong spatial coverage in the Northern Atlantic and Pacific ocean and by the scientific interest to study locations with strong current and sharp topography.

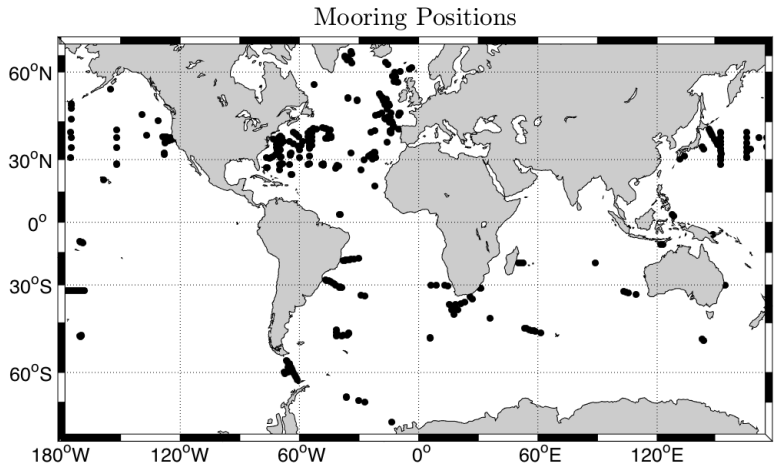

Figure 1: Positions of the moorings. The last update of the mooring collection was performed in Alford (2003). Our current study highlight the importance of gathering long term time series with a hour or less sampling frequency. Such observations allow to study the scale interactions that drive the KE cascade toward dissipation scales

Each of these moorings recorded the ocean velocities at multiple depths. The phase and amplitude of the observed currents are similar to the barotropic tides from the TPXO7.2 model (Egbert and Erofeeva (2002), figure 2). By removing the barotropic tidal currents from the data, we aim to estimate the level of KE in the IGW continuum.

In order to obtain a time evolution of the Fourier coefficients, a 30-days sliding window along the complex velocities time series is used to perform the sine multitaper method of Riedel and Sidorenko (1995). Following Alford and Whitmont (2007) who used the multi-taper method to study the near inertial peak behavior, we use $K = 3$ tapers. The method is applied at every time step and the resulting rotary spectra averaged over 24h.

In each individual time series, the time evolving spectra are used to define significant peaks at the near-inertial, diurnal and semi-diurnal tidal frequencies as well as their harmonics (linear combination of f and tidal components). The widths and positions of these peaks are defined for the entire time series using the time average and the standard deviation of the spectra in order to highlight the main and highly variable peaks (figure 3).

The IGW continuum is defined as the spectral KE distribution between f and N without these sources (NIW, IT and their harmonics). To investigate the dynamics of the IGW continuum, we perform a least square best fit of the GM79 spectrum by varying the level of KE in GM79. By default, this level E_{GM} is usually set at $2\pi \times 10^{-5}$ ($E0_{GM}$). This value defines the canonical GM79 spectrum and is chosen to fit a wide number of observations. This study completes the previous work by Hennon et al. (2014) who compare the variability of spectra observed with ARGO floats to the canonical GM79. Here, we intend to do the same comparison using a large set of global Eulerian observations.

It is important to notice that the level of KE in GM79 is also sensitive to the stratifica-

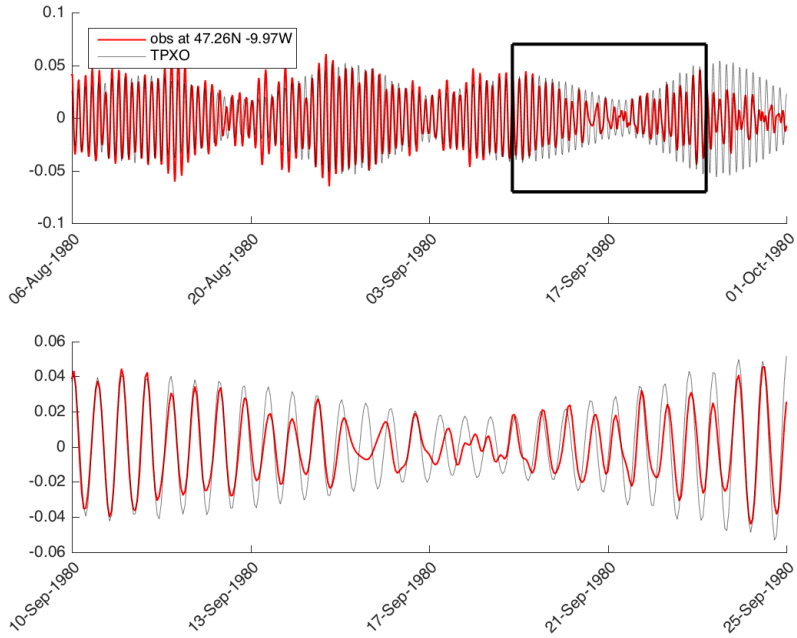

Figure 2: Top panel: Observed (red line) time series at 47.26 ° N 9.9 ° W and the TPXO barotropic tide estimation (black line). Bottom panel: zoom on a spring-neap tidal cycle of the above time series. In this study, the difference between both define the baroclinic velocities used to compute the time evolving spectra

tion. Here, we used an estimate of N given by the Levitus and Boyer (1994) climatology. As a consequence, the time averaged $\overline{E_{GM}}$ is strongly dependent on the accuracy of this product. The variability of E_{GM} is less sensible to the background stratification but is sensitive to the quality of the time series. The instruments have frequent failures that are easy to identify and correct in most cases. In these cases, only a few outliers behave like Dirac peaks. Such outliers tend to increase the high frequency KE and flatten the slope. An exhaustive quality control is still in progress. In this study we only the present 1757 controlled moorings.

2.1 Results

2.2 Dynamics of the internal wave continuum

The IGW continuum is an important pathway to the dissipation from energy sources like the wind, tides and likely a part of the meso/submesoscale activity. Consequently, if such a vision is valid, the variability of the KE level in the IGW continuum, characterized by E_{GM}, should be correlated with the variability of the sources. The time evolution of the KE within the NI peak, the tidal peaks or the mesoscale activity (defined as the low frequency of the 30 days spectrum) provide a good proxy to estimate the time evolution of the energy sources. These sources are obviously strongly variable in space too. Depending on the location, the relative influence of a source might change by several orders of magnitude. In the Kuroshio area (figure 4, top panel), the NI peak and the meso scale activity are frequently 10 times higher than the energy in the M2 tide. In the Celtic Sea (figure 4, bottom panel), the M2 tide is dominant and only the NI peak matches the

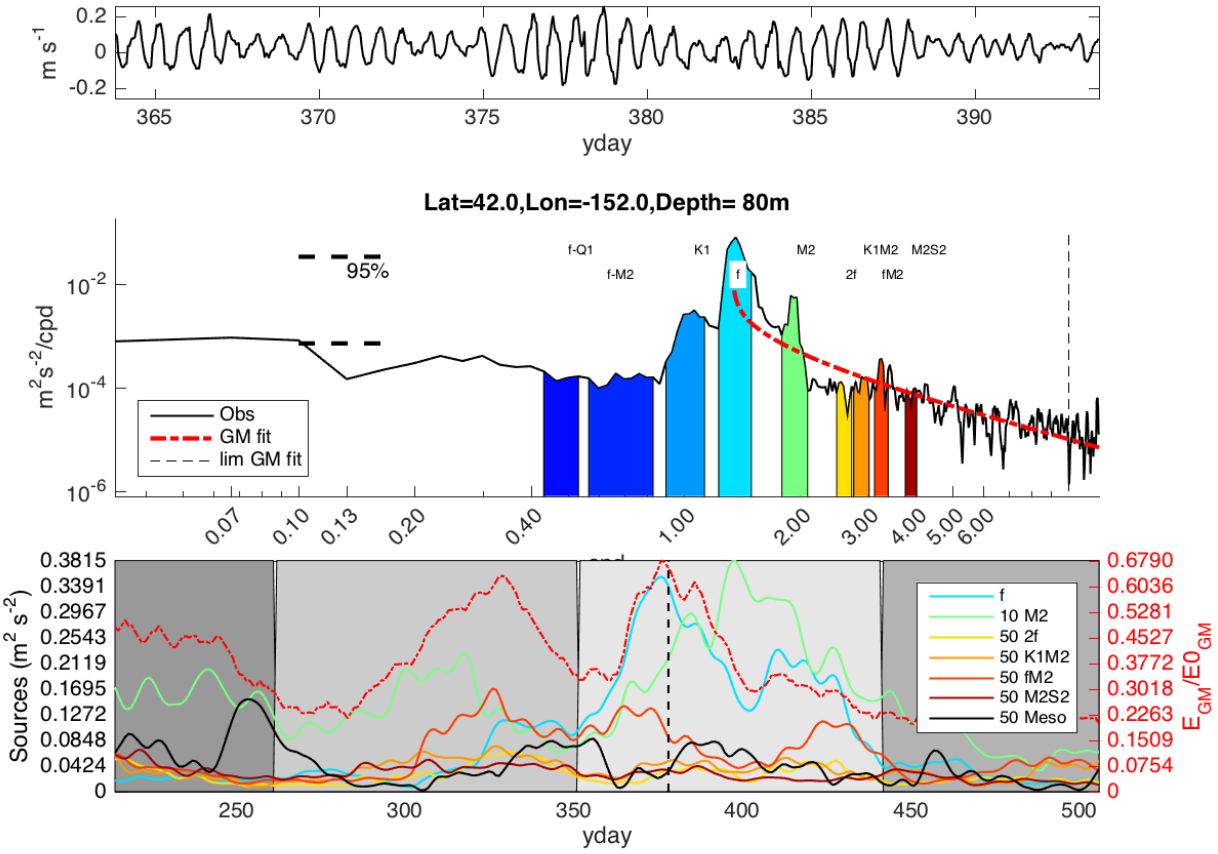

Figure 3: 30 days time series of a North Pacific mooring located at 42 °N and 152 °W (top panel) and the multi-tapered spectrum associated with this 30 days time series. The dashed red line correspond to the least square best fit of the GM spectrum. The colors correspond to the statistically major peaks among the sources (Near Inertial and Tidal peaks) and the black dashed line represent the highest frequency used to perform the least square best fit. The bottom panel shows the time evolution of the KE of these different peaks(same colors as above), the ratio between the GM best fit and the canonical GM spectrum (red dashed line) and the meso scale activity over the whole time series (black line). The meso scale activity is idealized as the lowest frequency of the spectrum. The black dashed line point out the instant defined by the two upper panels.The different shades of gray identify the different season

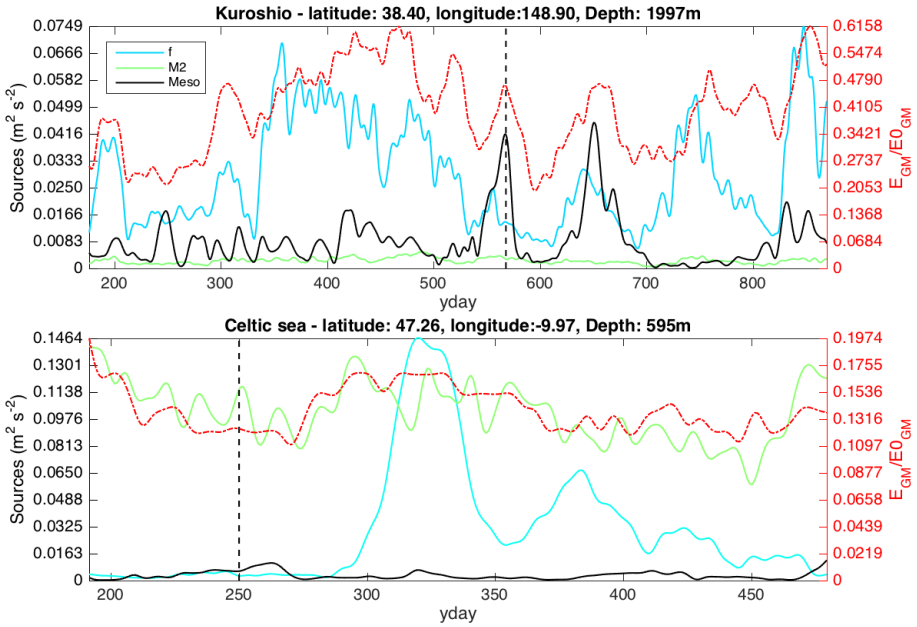

Figure 4: Time evolution of the KE within the near inertial (f) and M2 tide peaks and the mesoscale activity (blue, green and black line respectively) at location where the meso scale turbulence is strong (Kuroshio, top panel) and where the tides are strong (Celtic Sea, bottom panel). The black dashed line shows the time used to compute the spectra of the figure 5

M2 level of KE in winter time. The main source of KE differs for the three site described in this paper. The mesoscale, the IT and the NIW are the dominant dynamics at the Kuroshio, Celtic Sea and the Northern Pacific Ocean sites, respectively (figure 5).

The variability of E_{GM} clearly shows patterns similar to those observed for the dominant source of energy: NI peak for the Kuroshio mooring and M2 tides for the Celtic Sea. Next to the Kuroshio, some variations of E_{GM} seem correlated with the mesoscale activity (around year day 550). Despite the great similarity between E_{GM} and the NI peak or M2 tide variability, the behavior of E_{GM} does not follow a simple linear combination of the different sources. At year day 320, for the Celtic Sea mooring (figure 4, bottom panel), the rise of the NI peak does not influenced E_{GM}.

Explaining or simply documenting the relationship between E_{GM} and the sources is one of the goals of this ongoing study. Meanwhile, the great number of moorings available in this data set allows us to estimate the mean behavior of E_{GM} and its spatial and temporal variability.

2.3 Global variability of internal wave continuum

The global distribution of the time averaged $\overline{E_{GM}}$ (figure 6, top panel) is clustered around $E0_{GM}$, a value defined in GM79 forty years ago to fit with sparse observations. However, some values of $\overline{E_{GM}}$ are greater than $E0_{GM}$. These values can be explained by either a high KE level or the bias induced by the use of an inaccurate stratification. A high KE level might explain the high values observed in the Gulf stream and Kuroshio area. This is still under investigation. The variations of E_{GM} presented here (figure 6, bottom panel) show that the KE level in the IW continuum can vary up to a decade between

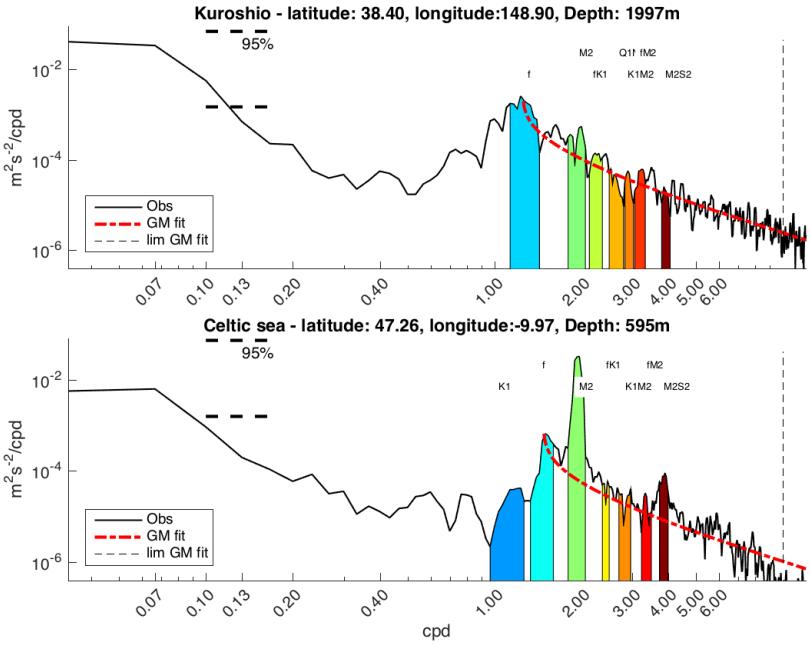

Figure 5: Kinetic energy Spectra near the Kuroshio (top panel) and in the Celtic Sea (bottom panel) at year 568 and 250 respectively. The colors identify the different main peaks over the whole time series.

its minimum and maximum values. This is particularly true near the Western boundary currents (Gulf stream, Kuroshio and Agulhas current).

This great variability of E_{GM} near areas with strong mesoscale turbulence suggests that meso and sub-mesoscale turbulence influence the high frequency part of the KE spectrum transferring energy either by interacting with internal wave or simply because a part of this turbulence shares the same time scale range.

3 Conclusions

The variability of the IGW continuum is studied using a large data set of long term Eulerian time series. Spectra are calculated along the time series in order to find the time evolution of the high frequency Fourier coefficients within the IGW continuum. With this method, we can perform a least square best fit of GM79 on these Fourier coefficients. The GM79 fit provides an estimate of the level of KE in the continuum (E_{GM}) which varies in time. As a first result of this study, the level of KE in the continuum varies in space and time about a decade at some locations, often around the canonical value $E0_{GM} = 2\pi \times 10^{-5}$ defined for GM79. The variations of E_{GM} seem to regularly follow the variations of the main energy source in the area (near inertial or tidal peak). However, the continuum behavior is more complex than a simple linear combination of the variations of the internal wave energy sources. Thorough a closer examination of all data, our analysis will document and provide statistics, on a global scale, of the time varying behavior of the internal wave field and its interaction with both the wind and the mesoscale activity.

References

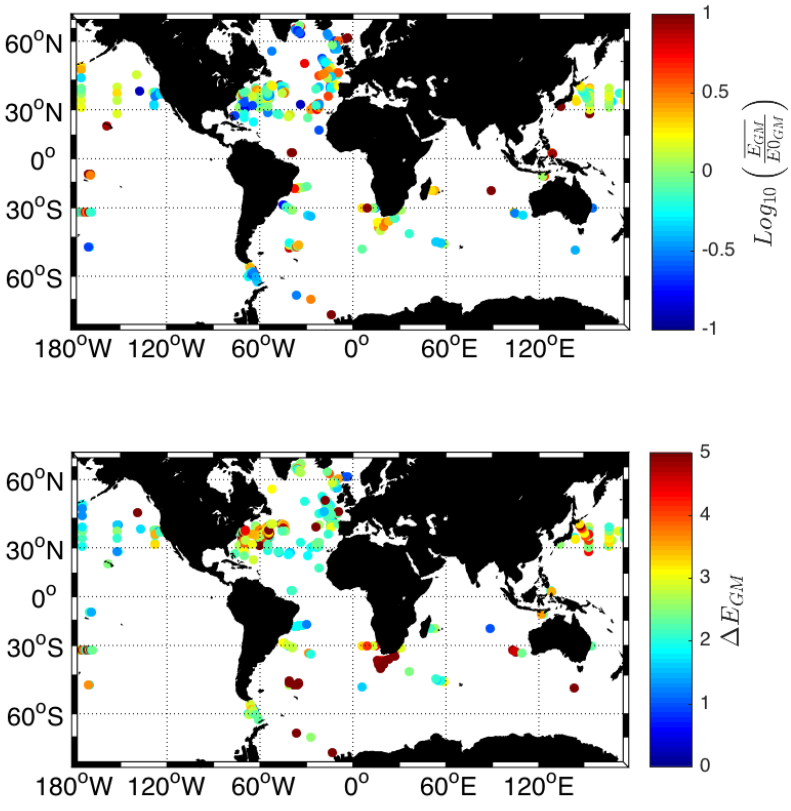

Figure 6: Log10 (top panel) of the time averaged of $\frac{E_{GM}}{E0_{GM}}$ and $\frac{max}{min} E_{GM}$(bottom panel)

Alford, M. H. (2003). Energy available for ocean mixing redistributed through long-range propagation of internal waves. *Nature*, 423:159–163.

Alford, M. H. and Whitmont, M. (2007). Seasonal and spatial variability of near-inertial kinetic energy from historical moored velocity records. *J. Phys. Oceanogr.*, 37(8):2022–2037.

Clement, L., Frajka-Williams, E., Sheen, K. L., Brearley, J. A., and Garabato, A. C. N. (2016). Generation of internal waves by eddies impinging on the western boundary of the north atlantic. *J. Phys. Oceanogr*, 46:1067–1079.

Egbert, G. and Erofeeva, S. (2002). Efficient inverse modeling of barotropic ocean tides. *J. Atmos. Ocean. Tech.*, 19:183–204.

Frankignoul, C. J. and Joyce, T. M. (1979). On internal wave variability during the Internal Wave Experiment (IWEX). *J. Geophys. Res.*, 84:769–776.

Garrett, C. and Munk, W. (1979). Internal waves in the ocean. *Ann. Rev. Fluid Mech.*, 11:339–369.

Gregg, M. (1989). Scaling turbulent dissipation in the thermocline. *J. Geophys. Res.*, 94(C7):9686–9698.

Hennon, T. D., Riser, S. C., and Alford, M. H. (2014). Observations of internal gravity waves by argo floats. *Journal of Physical Oceanography*, 44(9):2370–2386.

Henyey, F. S., Wright, J., and Flatté, S. M. (1986). Energy and action flow through the internal wave field. *J. Geophys. Res.*, 91(C7):8487–8495.

Levitus, S. and Boyer, T. (1994). *World Ocean Atlas 1994*. NOAA Atlas NESDIS 4, U.S. Department of Commerce, Washington, D.C.

Nikurashin, M. and Ferrari, R. (2010). Radiation and dissipation of internal waves generated by geostrophic motions impinging on small-scale topography: Theory. *J. Phys. Oceanogr.*, 40(5):1055–1074.

Nikurashin, M., Ferrari, R., Grisouard, N., and Polzin, K. (2014). The impact of finite-amplitude bottom topography on internal wave generation in the Southern Ocean. *J. Phys. Oceanogr.*, 44(11):2938–2950.

Pinkel, R. (1985). A wavenumber-frequency spectrum of upper ocean shear. *J. Phys. Oceanogr.*, 15:1453–1569.

Riedel, K. S. and Sidorenko, A. (1995). Minimum bias multiple taper spectral estimation. *IEEE Transactions on Signal Processing*, 43(1):188–195.

Watson, K. M. (1985). Interaction between internal waves and mesoscale flow. *J. Phys. Oceanogr*, 15:1296–1311.